FORMATION OF SURFACE NANOCRYSTALLINE STRUCTURE IN STEELS BY AIR BLAST SHOT PEENING

H. Saitoh 1, T. Ochi 1, M. Kubota 1

1 Muroran R&D Laboratory, Nippon Steel Corporation, 12 Nakamachi Muroran City Hokkaido 050-8550, Japan

ABSTRACT

The influences of steel hardness and shot peening (SP) conditions on the surface nanocrystalline layers produced by air blast SP was investigated with steels having Vickers hardness ranging from 260HV to 710HV. It was found that the easiness to form a nanocrystalline structure is related to steel hardness and SP conditions. Considering geometrically necessary (GN) dislocation density at surface of steel after SP, it can be said that the greater GN dislocation density at surface, the greater the amount of nanocrystalline layers and there is a critical GN dislocation density to form a nanocrystalline structure. The experimental results seem to support the dynamic continuous recrystallization mechanism rather than dynamic phase transformation mechanism.

KEY WORDS

shot peening, nanocrystalline structure, steel, surface, dislocation

INTRODUCTION

Shot peening (SP) has been widely used in order to improve the fatigue strength and stress corrosion resistance of industrial components, such as airplanes and automobiles, by adding compressive residual stresses in the near-surface regions of the components. Recent studies have reported that a nanocrystalline structure is formed by shot peening under some severe conditions (M. Umemoto, Y. Todaka, 2003) and the surface nanocrystalline structure results in further improvement of the fatigue strength of steels (T. Roland,2006, and Y. Todaka, 2006).

The nanocrystalline structure is said to be generated by severe plastic deformation processes: high-speed drilling (J. G. Li,2007), ball milling, high pressure torsion, a ball drop test, ultrasonic shot peening besides air blast SP (M. Umemoto, 2003). The formation mechanism of nanocrystalline formed by shot peening is attributed to dynamic continuous recrystallization in the alpha phase (Y. Xu, 2002 and H. Hidaka, 2003). On the other hand, during high-speed drilling dynamic phase transformation from the alpha to the gamma phase occurs, resulting in the formation of a nanocrystalline structure (M. Umemoto,2006).

In the previous studies half-width values measured by X-ray diffraction which are related to dislocation density were not used to discuss the necessary condition to form a nanocrystalline structure. In the present study, the surface nanocrystalline layers produced by air blast SP under various peening conditions are investigated with 0.5%C alloy steels of Vickers hardness ranging from 260HV to 710HV. By detailed characterization involving X-ray diffraction (XRD), a transmission electron microscope (TEM) and Vickers hardness testing, the conditions necessary to form a nanocrystalline structure are discussed.

METHODS

The chemical compositions of the steel bar product are listed in Table 1. The bar with a diameter of 35mm was normalized at 900°C for 1200s followed by air cooling. From this normalized bar, several test pieces named Q15, Q39, Q56, Q70, 8mm x 8mm x 60mm, were prepared as shown in Fig.1, while the Vickers hardness of the samples is listed in Table 2. SP was performed by air blast SP equipment (manufactured by Sintokogio Ltd.) at room temperature to these specimens, using rounded cut wire steel shot with a diameter of 1.0mm from a distance of 200mm. The hardness of the shot is 747HV, which is harder than the hardest specimen Q15. The SP conditions are shown in Table 3.

Table 1. Chemical compositions of specimen used (mass%)

C	Si	Mn	P	S	T-Al	Cr	Mo	T-N
0.52	0.24	0.75	0.016	0.026	0.023	1.0	0.16	0.0050

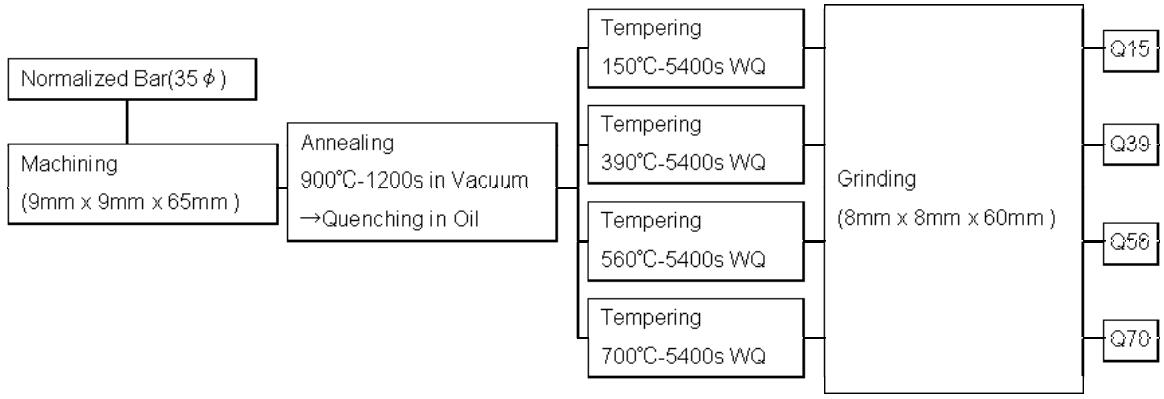

Fig.1. Sample preparation before shot peening.

Table 2. Vickers hardness of specimens.

Specimens	Q15	Q39	Q56	Q70
HV10	711	515	371	263

Table 3. Conditions of shot peening.

Conditions	1	2	3	4
Shot velocity (m/s)	30	30	90	90
Blasting pressure (MPa)	0.1	0.1	0.5	0.5
Coverage (%)	300	3,000	300	3,000
SP duration(s)	12	120	12	120

The shot peened specimens were characterized by an optical microscope (OM), a TEM(HITACHI HF-2000 operated at 200KV), X-ray diffraction, and a Vickers microhardness tester. The specimens etched by 5% Nital were observed by an OM. The TEM samples in the SP experiments were prepared parallel to the shot-peened surface of the specimens. The half-width values of the specimens were determined with CrKα-radiation the {211}-interference lines. The depth distributions of the half-width values were determined by electrolytic removal of thin surface layers and subsequent X-ray measurements. The surface texture of each specimen was estimated by roughness Ry(JIS B0601 1994) using a contact (stylus) instrument and by a scanning electron microscope (SEM).

RESULTS

Morphology of the nanocrystalline layers

The cross-sectional OM images of the so-called white etching layers (WELs) at the surface of the shot-peened specimens are shown in Fig.2. There are two types of WELs; one of which is a “string-like WEL” and the other a “cloud-like WEL”. In the hardest specimen Q15, only the string-like WELs are observed under all four SP conditions. The Vickers hardness of the WELs in the four specimens under SP condition 1 was tested by a microhardness tester (load: 0.098N), resulting in 800HV ～1000HV. Figure 3 shows the TEM dark field image and the corresponding selected area diffraction (SAD) rings, taken from the top surface region in the specimen Q15 (SP condition 4). The image shows that the structure of the nanocrystalline region consists of grains of diameter 10～100nm in size. The SAD rings indicate that the grains are bcc-ferrite (which could not be distinct from the martensite phase) and randomly oriented. Based on these characteristics, the WELs can be said to be nanocrystalline layers.

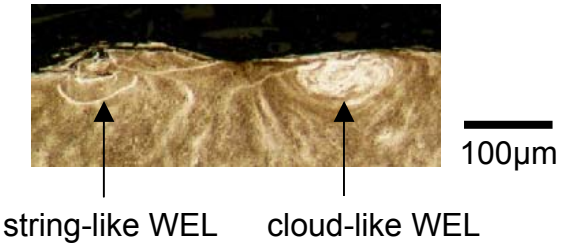

Fig.2. OM image of WEL (Q39, SP condition 4).

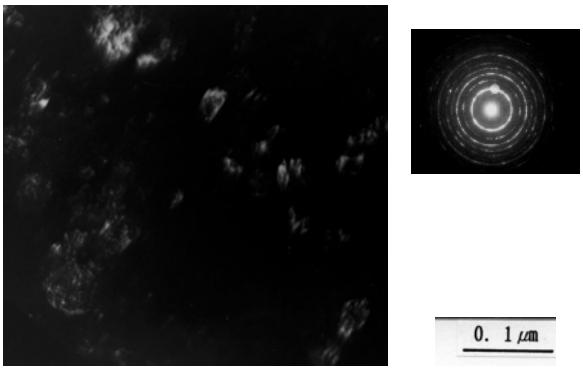

Fig.3. Dark field image and SAD of WEL (Q15, SP condition 4).

Influence of the steel hardness and SP conditions on the formation of nanocrystalline layers

The amount of nanocrystalline layers formed by SP changes depending on the specimen’s hardness and the SP conditions. As the amount of nanocrystalline layers, the percentage of nanocrystalline layers covering the surface* was measured for all the specimens. As shown in Fig.4, under the weakest SP condition (SP1) no WELs are observed in the softest specimen Q70. Under the same SP processing duration, the faster the shot velocity, the greater the percentage of nanocrystalline layers. Under the same shot velocity, the longer the SP processing duration, the greater the percentage of nanocrystalline layers.

*Observing all the surface of the cross-sectional OM images, we have measured the each length parallel to the surface of the areas where the WELs exist. The ratio of these total lengths to the specimen’s surface length was defined as the percentage of nanocrystalline layers.

DISCUSSION

Takaki (S. Takaki,2006) reported that the repeatedly folding of the deformed regions leads to the formation of cloud-like WELs in softer steels(≤HV3.72GPa). From this standpoint the surface roughness of each specimen was examined(Fig.5). Before SP the surface roughness Ry is 2～4μm. The typical surface SEM images corresponding to Fig.5 are shown in Fig.6. The surface textures of Q56, Q39 are similar to Q70. In the present study cloud-like WELs are observed in specimens of

hardness less than 515HV and are not observed in Q15. Therefore, the repeatedly folding deformation occurs in the specimens with the hardness less than 515HV, resulting in larger surface roughness. Comparing Fig.5 with Fig.4, especially SP condition 1, Q39 and Q56 (folding mechanism) are easier to form a nanocrystalline structure than Q70 and Q15. The easiness to form a nanocrystalline structure is assumed to relate to the hardness of the specimens and SP conditions rather than deformation modes.

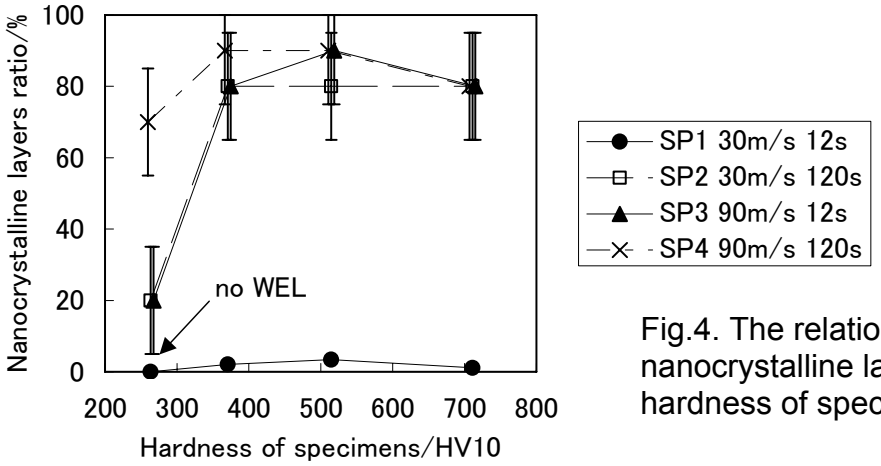

Fig.4. The relationship between nanocrystalline layers ratio and the hardness of specimens.

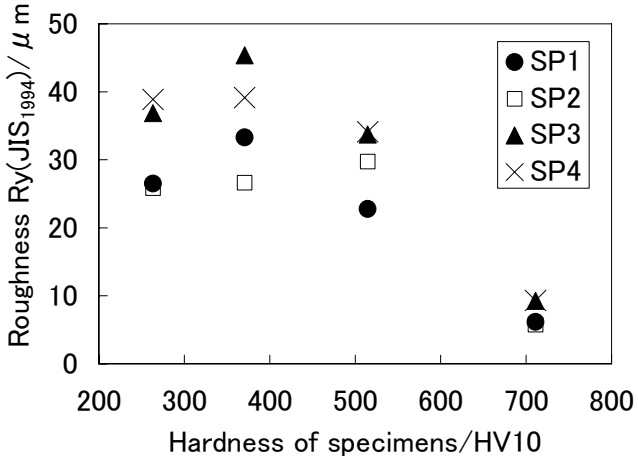

Fig.5. Surface roughness of each specimen after SP.

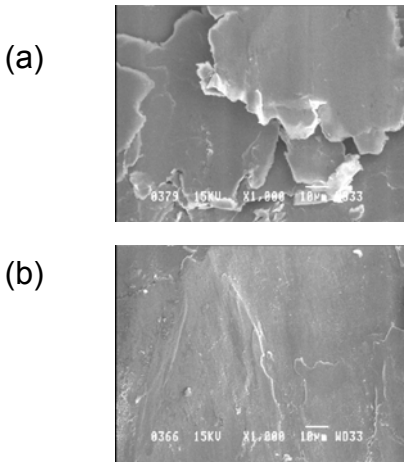

Fig.6. Surface SEM iamges after SP. (a) Q70(SP3) and (b) Q15(SP3).

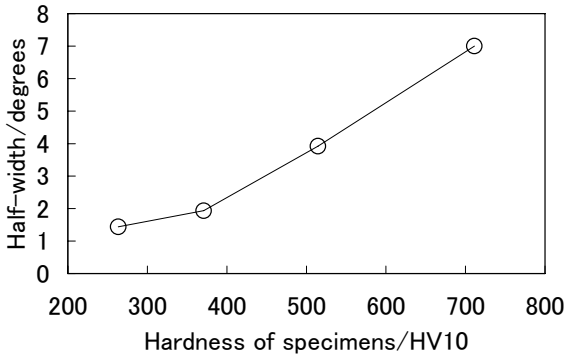

Fig.7. Relationship between half-width value and hardness of each specimen.

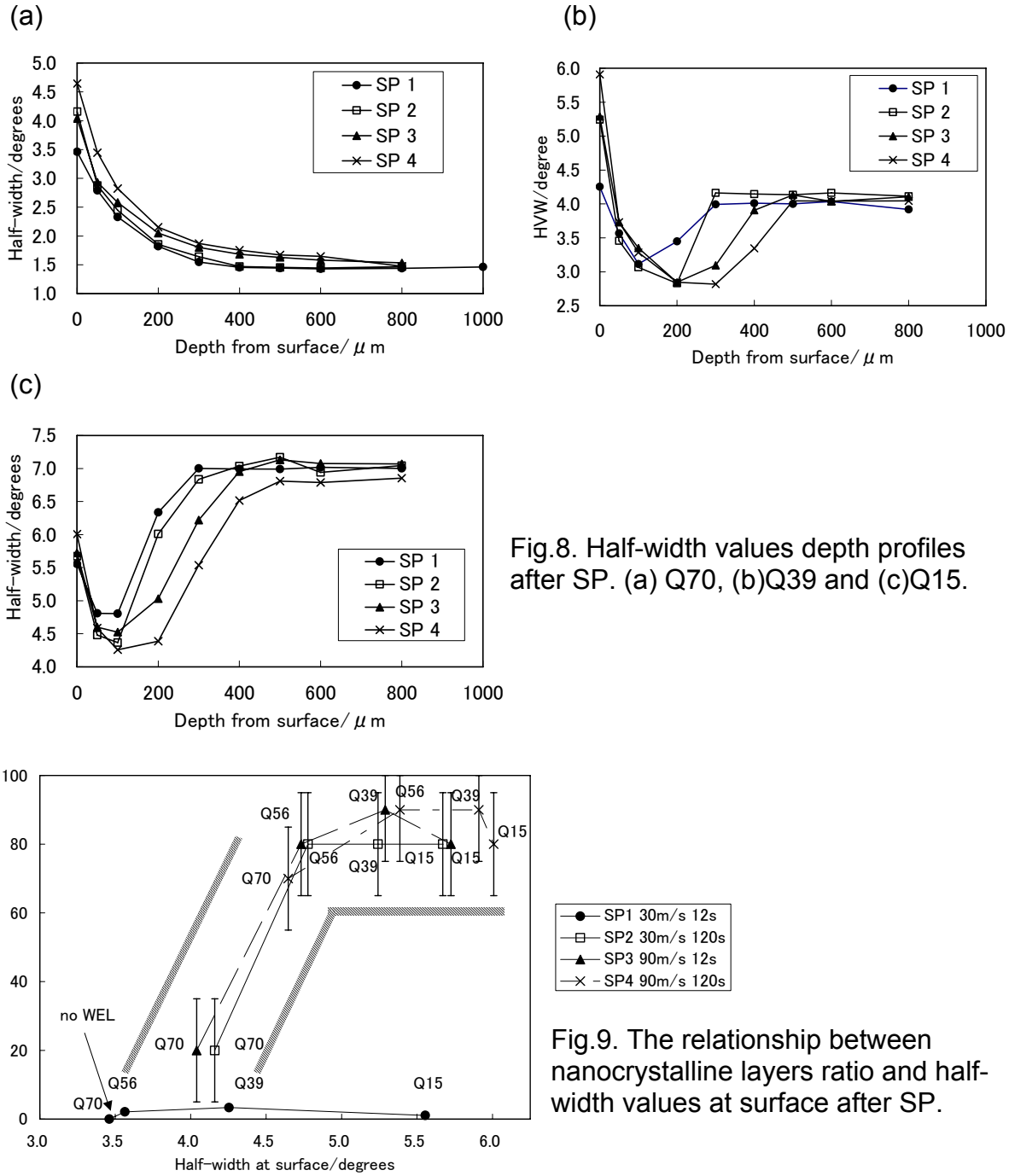

Fig.8. Half-width values depth profiles after SP. (a) Q70, (b)Q39 and (c)Q15.

Fig.9. The relationship between nanocrystalline layers ratio and half-width values at surface after SP.

The relation between the hardness and the half-width value at the depth of 800μm, which is not affected by SP, of each specimen is shown in Fig.7. Since a half-width value is said to be proportional to dislocation density(K. Nakajima,2004), the harder the specimens, the higher the dislocation density. Figure 8 shows the half-width values depth profiles of Q70, Q39 and Q15 after SP. In specimen Q70, a continuous increase of the half-width values is observed, peaking at the surface. The depth distribution of Q56 is similar to Q70. The half-width value of specimen Q39 also peaks at the surface while the minimum half-width value occurs approximately 200μm below the surface. In specimen Q15 the minimum half-width value is observed at about 100μm below the surface and the half-width value at the surface is not the maximum. Steels with a low dislocation density increase their dislocations by SP, leading to the formation of a nanocrystalline structure at the surface. On the other hand, in steels with a high dislocation density, a minimum half-width value at 100～200μm below the surface seems to result from the

annihilation of the original statistically stored (SS) dislocations having opposite signs moved by the shear stresses which are induced by SP. The surface dislocation density after SP is presumed a more important factor to form a nanocrystalline structure rather than the original dislocation density before SP. Changing the horizontal axis of Fig. 4, Fig.9 is obtained.

From Fig.8(c), in specimen Q15 under SP condition 1, the annihilation of SS dislocations seems insufficient, resulting in remaining of many SS dislocations. Therefore, in this specimen the half-width value at the surface contributed by GN dislocations is presumed to be smaller. Figure 9 seems to suggest that the greater GN dislocation density at the surface, the greater the amount of nanocrystalline layers and there is a critical GN dislocation density to form a nanocrystalline structure. The above experimental results seem to support dynamic continuous recrytstallization mechanism (Y. Xu,2003) rather than dynamic phase transformation mechanism.

CONCLUSIONS

The surface nanocrystalline layers produced by air blast SP with various peening conditions are investigated with 0.5%C alloy steels of Vickers hardness ranging from 260HV to 710HV. The results obtained are summarized as follows.

(1) Under the same SP processing duration the faster the shot velocity, the greater the amount of nanocrystalline layers.
(2) Under the same shot velocity, the longer the SP processing duration, the greater the amount of nanocrystalline layers.
(3) The easiness to form a nanocrystalline structure is related to steel hardness and SP conditions. Considering GN dislocation density at surface of steel after SP, it can be said that the greater GN dislocation density at surface, the greater the amount of nanocrystalline layers and there is a critical GN dislocation density to form a nanocrystalline structure.
(4) The experimental results seem to support the dynamic continuous recrystallization mechanism rather than dynamic phase transformation mechanism.

REFERENCES

H. Hidaka, K. Kawasaki, T. Tsuchiyama, S. Takaki : Mater Trans. 44 (2003) p.1912-1918

Nakajima, Y. Futamura, H. Hidaka, S. Tsuchiyama, S. Takaki: CAMP-ISIJ 17 (2004) p.396-399

J. G. Li, M. Umemoto, Y. Todaka, K. Tsuchiya: Acta Mater 55 (2007) p.1397-1406

T. Roland, D. Retraint, K. Lu, J. Lu: Scrip. Mater. 54 (2006) p.1949-1954

S. Takaki, M. Kumagai, Y. Ito, S. Konuma, E. Shimodaira: Tetsu-to-Hagané 92 (2006) p.318-326

Y. Todaka, M. Umemoto, J. G. Li, Y. Kawabata, K. Tsuchiya: CAMP-ISIJ 19 (2006) p.1339

M. Umemoto, Y. Todaka, K. Tsuchiya: Materials Transactions 44 (2003) p.1488-1493

M. Umemoto: Materials Transactions 44 (2003) p.1900-1911

M. Umemoto, Y. Todaka, J. G. Li, , K. Tsuchiya :Mater. Sci. Forum 503-504 (2006) p.11-18

Y. Xu, Z. G. Liu, M. Umemoto, K. Tsuchiya: Metall. Mater. Trans. A 33A (2002) p.2195-2203